Oxidation and Sulfidation Resistant Alloys with Silicon Additions

J.S. Dunning and D.E. Alman
U.S. DOE, Albany Research Center, 1450 Queen Avenue, SW, Albany, OR 97321
E-mail: dunning@alrc.doe.gov Telephone: 541-967-5876; Fax: (541) 967-5845

J.A. Poston, Jr. and R. Siriwardane, U.S. DOE, National Energy Technology Laboratory

The Albany Research Center (ARC) has considerable experience in developing lean chromium, austenitic stainless steels with improved high temperature oxidation resistance. Using basic alloy design principles, a baseline composition of Fe-16Cr-16Ni-2Mn-1Mo alloys with Si and Al addition at a maximum of 5 weight percent was selected for potential application at temperatures above 700ºC for supercritical and ultra-supercritical power plant application. The alloys were fully austenitic. Cyclic oxidation tests in air for 1000 hours were carried out on alloys with Si only or combined Si and Al additions in the temperature range 700ºC to 800ºC. Oxidation resistances of alloys with Si only additions were outstanding, particularly at 800ºC (i.e., these alloys possessed weight gains 4 times less than a standard type-304 alloy). In addition, Si alloys pre-oxidized at 800ºC, showed a zero weight gain in subsequent testing for 1000 hours at 700ºC. Similar improvements were observed for Si only alloy after H_2S exposure at 700ºC compared with type 304 stainless steel. SEM and ESCA analysis of the oxide films and base material at the oxide/base metal interface were conducted to study potential rate controlling mechanisms at ARC. Depth profile analysis and element concentration profiles (argon ion etching/x-ray photoelectron spectroscopy) were conducted on oxidized specimens and base material at the National Energy Technology Laboratory.

INTRODUCTION

The oxidation resistance in Fe-Cr-Ni alloys containing greater than 16 wt. pct. Cr is considered to be due to the formation of tightly adherent chromia (Cr_2O_3) films at the surface. The rate controlling mechanism of oxidation is attributed to the outward diffusion of metal ions[1,2]. Grain boundary diffusion is an important factor. It is also known that relatively minor additions of Al and Si can play a significant role in the oxidation process of Fe-Cr-Ni alloys. Small additions of Si have been reported to have a beneficial effect on oxidation resistance due to the formation of SiO_2 at the metal/oxide interface[3-6]. The role of silicon is typically attributed to the formation of a silicon oxide layer between the oxide and metal interface. The formation of chromia protective scales is promoted by this continuous or non-continuous silicon oxide layer that is reported to act as a diffusion barrier to Fe and Cr reaching the oxide layer. In some studies, the effect of Si is attributed to the formation of a continuous silica layer between the metal and the external chromia scale[7], although it is difficult to physically confirm a continuous, rather than non-continuous layer. Alloys with both Si and Al additions added have reported positive synergistic effects of the Si and Al additions on oxidation resistance[8,9].

All commercial Fe-based austenitic stainless steels contain about 0.5% Si and 1-2% Mn as residual impurities. In this study, a base composition of Fe-16Cr-16Ni-2Mn-1Mo was chosen. Mo is unique in providing high temperature strength and corrosion resistance. High purity Si additions of up to 3 wt. pct. were made to study the effect of these additions. In addition, alloys with both high purity Si and Al additions in combination were studied.

EXPERIMENTAL PROCEDURES

The Fe-16Cr-16Ni-2Mn-1Mo-Si and Fe-16Cr-16Ni-2Mn-1Mo-Si-Al alloys were produced by vacuum induction melting of 5 kg charges. High purity (99.9 pct. +) materials were used in the charges. The ingots were scalped, cleaned and forged and rolled to 12.7 mm sheet at 1075°C. The sheet material was annealed for 1 hour at 1200°C and air-cooled.

The alloy composition was designed to produce fully austenitic alloys with a combined silicon and aluminum content not to exceed 5 wt. pct. The onset of δ ferrite formation was predicted using the concept of Cr equivalence for multi-component alloys. In this research, the Cr and Ni equivalence equations of Schneider and Pickering were used together with a Cr equivalence equation. Thus, for the

$$\text{Cr eq} = \text{Cr} + 1.5\,\text{Mo} + \text{Si} + 1.5\,\text{Al}$$

$$\text{Ni eq} = \text{Ni} + 0.5\,\text{Mn}$$

and

$$\text{net Cr eq} = \text{Cr eq} - 0.691\,\text{Ni eq}$$

δ ferrite formation occurs when net Cr eq < 10 percent.

The coefficients ahead of each alloying element are very composition sensitive and the coefficients for Si and Al in the above equations were selected and used specifically for the 16 Cr, 16 Ni base composition.

Samples for oxidation studies were cut from the 12.7 mm annealed sheet. Samples with nominal dimensions of 25.4 x 25.4 x 7.6 mm were machined and polished to a 400-grit finish. Cyclic oxidation tests were carried out at 700°C and 800°C in a tube furnace. Weight changes were recorded at regular intervals after removing samples from the furnace and cooling to room temperature.

Chemical compositions were determined by wet chemical analysis and phase analysis was conducted by x-ray diffraction (XRD). Local elemental analysis of the oxide films and the bulk metal at the interface were conducted by electron spectroscopy for chemical analysis (ESCA).

A bromine-etching technique and scanning electron microscopy (SEM) were used to study the morphology of the oxide films at the oxide/metal interface. In this technique, the oxidized specimen is mounted in epoxy and ground on an angle to expose the metal specimen. An alcohol/bromine solution is dripped onto the metal until it is dissolved to expose the back surface of the oxide scale at the metal/oxide interface for subsequent examination in the SEM.

Depth profile analysis (argon ion etching/x-ray photoelectron spectroscopy) was conducted on a series of Fe-16Cr-16Ni-2Mn-1Mo with 2Si stainless steel samples oxidized at 700ºC and 800ºC for resonance times of 25 hours, 100 hours, 193 hours, 436 hours and 700 hours.

RESULTS AND DISCUSSION

Table I shows the nominal composition of the charges melted and rolled to plate. Cyclic oxidation tests were conducted at 700°C and 800°C in air. Specimens of a conventional 18Cr-8Ni type 304 stainless steel were included as a standard. Results for the 1000-hour tests at

Table I. Nominal Composition (wt. pct.)

Alloy	Fe	Cr	Ni	Mn	Mo	Si	Al
A	Bal.	16	16	2	1	0	0
B	Bal.	16	16	2	1	3	0
C	Bal.	16	16	2	1	3	1
D	Bal.	16	16	2	1	2	0
E	Bal.	16	16	2	1	2	1
F	Bal.	16	16	2	1	2	2
G	Bal.	16	16	2	1	1	1

700°C are shown in Figure 1. The baseline Fe-16Cr-16Ni-2Mn-1Mo composition shows the highest rate of oxidation, which is significantly higher than the higher chromium 18Cr-8Ni standard. Alloys with Si only additions (Group B alloys) and Si combined with Al additions (Group A alloys) both showed weight gains approximately half that of the 18Cr-8Ni alloy. All data for Group A and Group B fell within the boundary curves shown in Figure 1 for these alloys. All alloys in Group A and Group B show a significant improvement (approximately 2 times in terms of weight gain) in oxidation resistance compared with the higher Cr type 304 stainless steel.

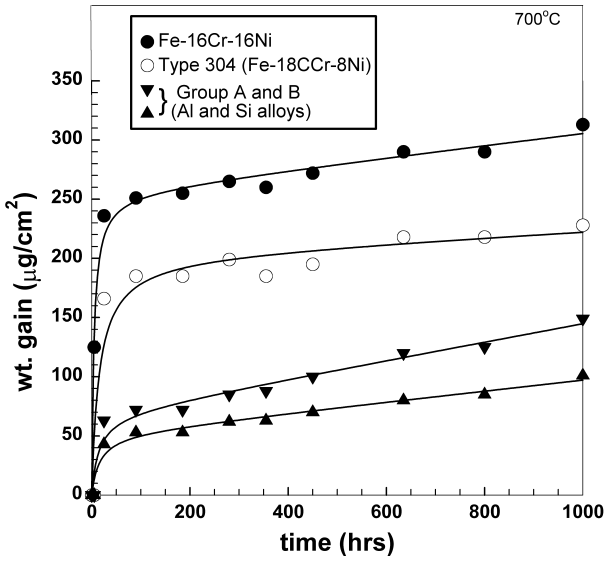

Figure 1. Oxidation behavior at 700°C.

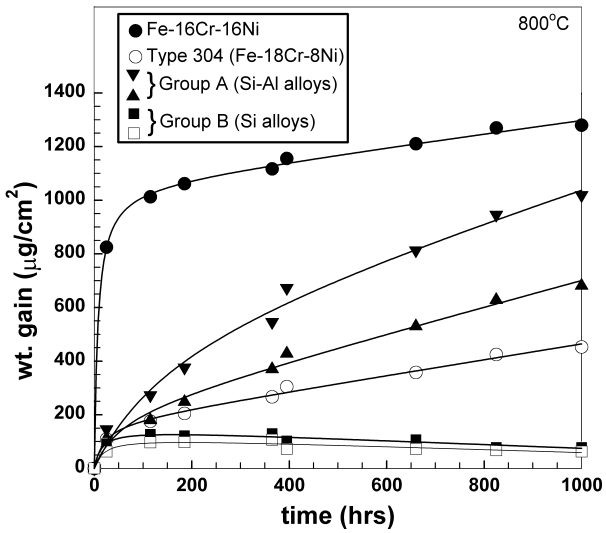

Figure 2. Oxidation behavior at 800°C.

Figure 2 shows results for cyclic oxidation at 800°C for the same alloy series. The first point to note is that Group A alloys (Si plus Al) and Group B (Si only) alloys behave differently at 800°C. Group A alloys show weight gains approximately 2 times greater than the standard type 304 alloy (18Cr-8Ni) while Group B alloys show weight gains 4 times less after 1000 hours at 800°C. Clearly, at 800°C, different oxidation mechanisms are operative in Group A (Si + Al) and Group B alloys (Si). It is evident that Si is very effective in providing oxidation protection at 800°C. Aluminum additions disrupt this effectiveness at 800°C.

The two Group B alloys with 2 percent Si and 3 percent Si additions were oxidized for 175 hours at 800°C prior to a 1000 hour exposure at 700°C together with standard type 304 stainless and Group B alloy specimens that had not been pre-oxidized. Data is shown in Figure 3. The Group B alloys (not pre-oxidized) and the type 304 standard showed the same relationship as the earlier 700°C tests. However, the pre-oxidized specimens showed zero weight gain after 1000 hours at 700°C.

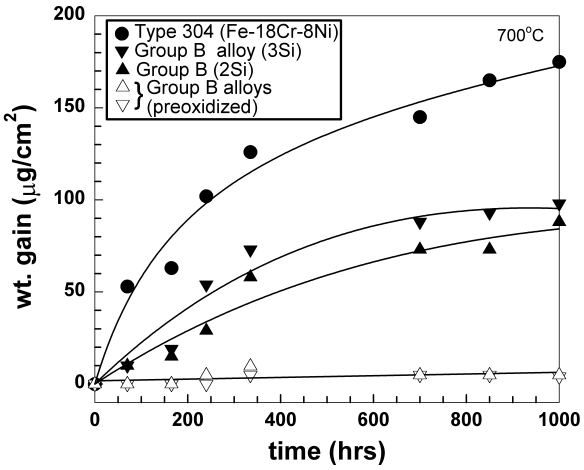

Figure 3. Oxidation behavior of pre-oxidized and non-pre-oxidized alloys at 700°C.

Table II shows an ESCA analysis of material at the oxide-metal interface for a Group B alloy (3Si) after a 1000-hour exposure at 800°C. Analyses of the bulk material is shown together with analyses close to the interface of the base metal and the oxide film. Analyses are shown in atomic percent for each element detected and is broken down into atomic percent at various binding energies. As a rule, the lowest binding energy observed indicates the elemental metal while higher binding energies represent oxides of varying complexity. In both alloys, the oxide is rich in Cr and Mn leading to a corresponding depletion of Cr and Mn in the base metal close to the interface. In the case of Mn, the depletion is almost complete. In the Si only alloy, a significant buildup of elemental Si occurs in the base metal near the interface (10.6 atomic pct. vs. 5.6 atomic pct. in the bulk metal). A smaller percentage of silicon is observed in the oxide film as an oxide.

Table II: ESCA Data for 2Si-2Al Alloy at 800°C

ELEMENT	NOMINAL ALLOY COMPOSITION (ATOMIC%)	ESCA ANALYSIS			
		CORRESPONDING BINDING ENERGY	COMPOSITION (ATOMIC%)		COMMENTS
			BASE METAL	OXIDE FILM	
FE	57.3	Elemental Fe	29.2	2.7	Low Fe conc., near interface reflect conc. in base metal of silicon, aluminum, oxygen, carbon
		Fe-Oxide	7.1	1.7	
CR	16.5	Elemental Cr	8.1		Cr depletion in base, heavy concentration in oxide film
		Cr-Oxide	1.5	21.0	
NI	14.8	Elemental Ni	6.7	1.2	No significance
		Ni-Oxide			
MN	2.2	Elemental Mn			Complete Mn depletion in base near interface, heavy concentration in oxide film
		Mn-Oxide	0	9.0	
MO	0.6	Elemental Mo	1.3	0.2	No significance
		Mo-Oxide			
SI	3.96	Elemental Si	9.6	1.0	Si concentration in base metal near interface
		Si-Oxide		4.5	
AL	4.4	Elemental Al			Al concentration as oxide in base metal near interface
		Al-Oxide	14.8	2.3	
O	-		16.7	48.8	
C	-		5.1	4.3	No significance. Buildup of C data typical of ESCA

As shown by these analyses, a feature of oxidation in the Fe-Cr-Si alloys is the Fe, Cr-oxide growth, and the eventual concentration of the interface of the minor alloying element Si. The overwhelming

presence of the Fe or Fe-Cr oxide inhibits or delays the ability of the minor elements to form oxide phase. The rate of diffusion of Si through the Fe base alloy and Fe, Cr oxides is slow. The Si ions remain in the base alloy at the metal/oxide interface as major elements of the alloy diffuse away and oxidize. As oxidation proceeds, the resulting higher concentrations of Si may now result in the formation of oxides not seen during the early stages of oxidation.

It is evident that Si only additions provide superior oxidation resistance at 800°C while the presence of Al disrupts this mechanism. The exact mechanism by which Si enhances oxidation resistance is a matter of some conjecture. The effect of silicon is clearly due to the concentration of Si at the interface and is usually attributed to a layer of silica (SiO_2) adjacent to the metal[10]. Claims are for a continuous or non-continuous film but physical evidence of a continuous film is difficult to provide. It has been suggested that the film acts as a diffusion barrier[11] or as a structure favoring the formation of thin, pure layers of chromia[12]. The outward diffusion of chromium through either the silica or the chromia layers controls the rate of oxidation.

The current study utilized a bromine etching technique to directly view the underside of the oxide film at the metal/oxide interface and suggested a different mechanism to explain the effect of small Si additions on the oxidation process. The etching technique removes all metal revealing the underside of oxide film at the metal/oxide interface.

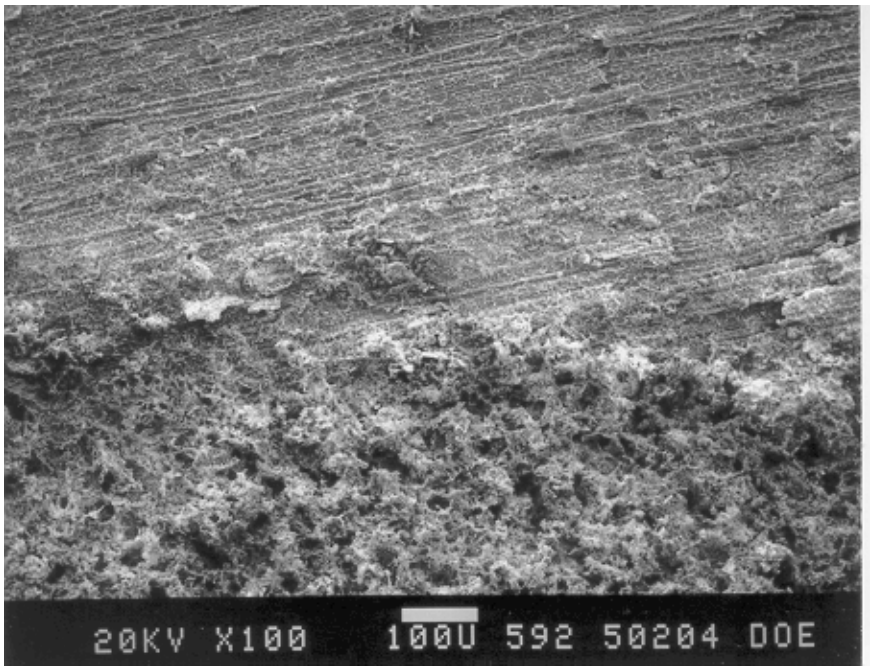

Figure 4. SEM micrograph of 3Si alloy pre-oxidized at 800°C followed by 1000 hours at 700°C. Transition between oxide (top) and metal (bottom) after bromine/alcohol etch.

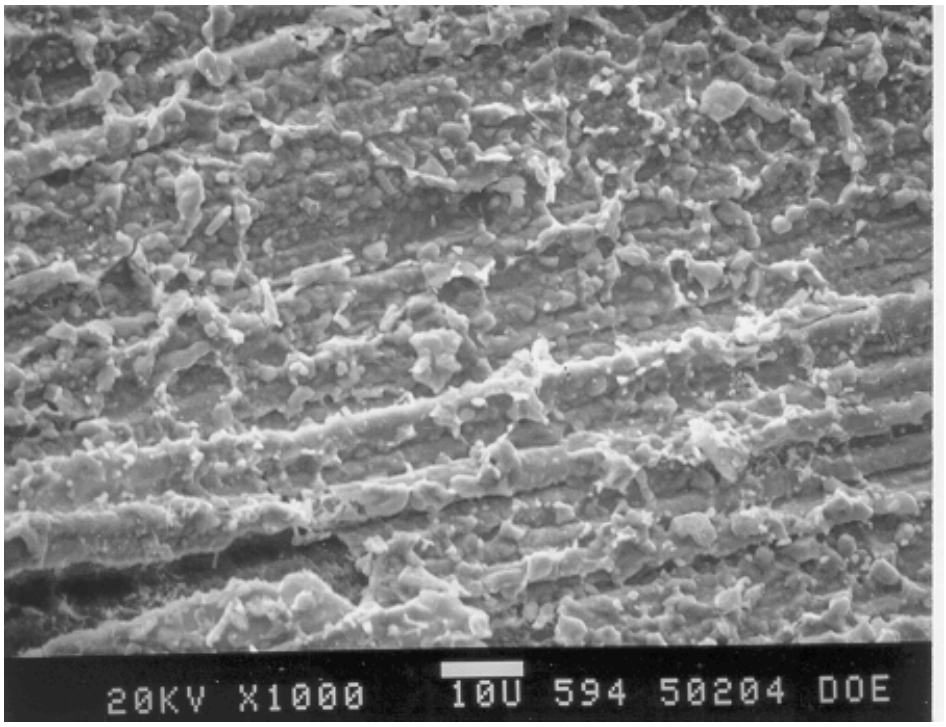

Figure 5. SEM micrograph of 3Si alloy showing oxide characteristics.

Figures 4 and 5 show the 3Si alloy (Table VI) after pre-oxidation of 175 hours at 800°C followed by 1000 hours exposure at 700°C. Figure 4 is a low magnification SEM micrograph of the interface between oxide film where the metal has been etched off by the bromine etch and an area where metal still remains. In the oxide film, the surface scratches of the 400 grit polish put on the oxidation specimens are replicated confirming the fact that the oxide at the metal/oxide is being viewed. At higher magnification, a grain boundary network of SiO_2 can be seen. Figures 6 and 7 show the SEM micrographs for the 2Si alloy with 1000 hours exposure at 800°C. In the 2Si alloy, the SiO_2 networks are more clearly developed with the specimen exposed for 1000 hours at 800°C having a well developed grain boundary network of SiO_2 with SiO_2 pegs at grain boundary triple points. These SiO_2 pegs extended into the metal from the metal/oxide interface. The intragranular oxide between the grain boundary networks is high in chromium. For specimens with 3Si-1Al and 2Si-2Al additions, the microstructure of the oxide film at the metal/oxide interface is entirely different. The surface of the oxide shows no indication of grain boundary oxide networks and the oxide analysis is lower in chromium.

The data suggests that the effect of Si, in the absence of Al additions, can be attributed to formation of Si oxide networks at the grain boundaries that significantly slow the outward diffusion of metal ions and favor the formation of a thin, pure chromia protective film. The presence of Al with a high oxidation potential evidently disrupts the formation of the Si oxide grain boundary networks.

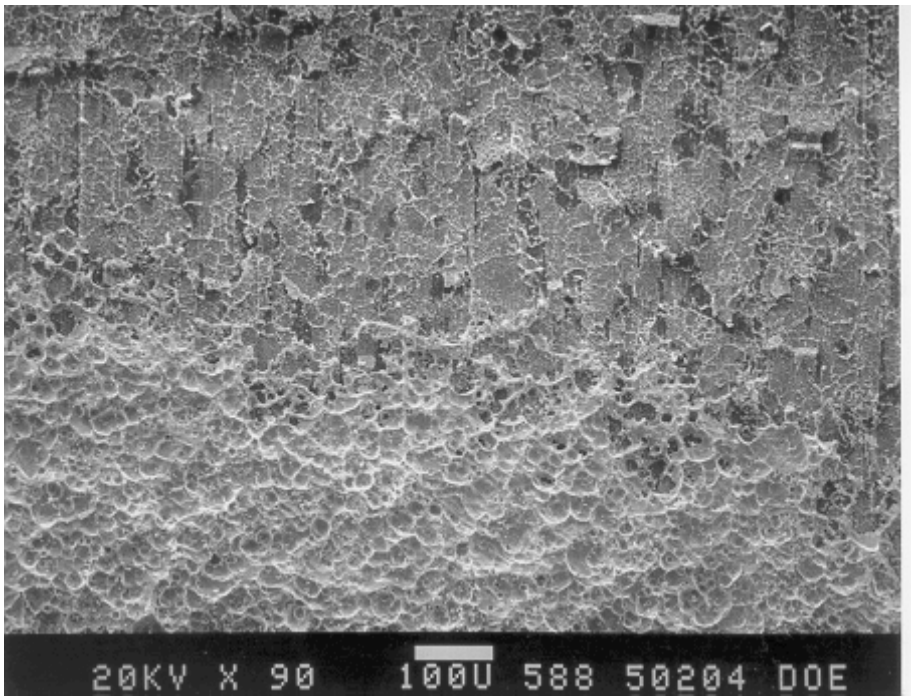

Figure 6. SEM micrograph of 2Si alloy after pre-oxidation at 800°C followed by 1000 hours at 700°C. Transition between oxide (top) and metal after bromine/alcohol etch.

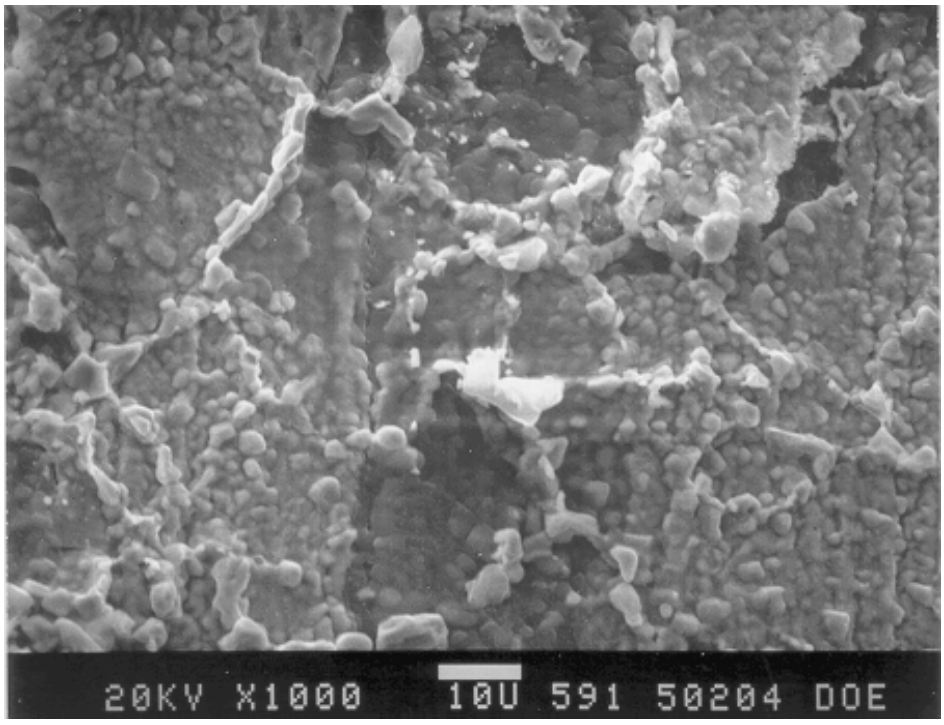

Figure 7. SEM micrograph of 2Si alloy showing oxide characteristics.

Depth profile analysis (argon etching/x-ray photoelectron spectroscopy) was conducted on 2Si specimens oxidized at 700ºC and 800ºC for 25 hours, 100 hours, 193 hours, 436 hours and 700 hours. These studies were conducted at the Department of Energy, National Energy Technology Laboratory (NETL). The results showed similar movement of elements to the ESCA studies reported in this paper. Mn depletion was noted at the metal-oxide interface with high manganese participation in the oxide film. Si was not active in the oxide film but was observed to increase toward the oxide-metal interface.

CONCLUSIONS

- A significant change in rate controlling mechanism in the oxidation of lean chromium alloys with Si additions occurs in alloys oxidized at 700°C and the same alloys oxidized at 800°C.
- Oxidation characteristics in alloys with Si additions are excellent at 800°C.
- These oxidation characteristics at 800°C are disrupted by small Al additions.
- Alloys with Si additions, pre-oxidized at 800°C, show no significant weight gain during subsequent 1000-hour oxidation tests at 700°C.
- SEM and ESCA studies suggest that the effect of minor Si addition on oxidation resistance at 800°C may be associated with grain boundary networks of SiO_2.

REFERENCES

1. H.E. Evans, D.A. Hilton and R.A. Holm, *Oxidation of Metals* **10**, 149 (1976).
2. B.D. Bastow, D.P. Whittle and G.C. Wood, *Oxidation of Metals* **12**, 413 (1978).
3. T. Morin and M. Rigaud, *Can. Metall. Q.* **9**, 521 (1970).
4. D.W. Bridges, J.P. Baur, G.S. Baur and W.M. Fassel, *J. Electrochem. Soc.* **103**, 475 (1956).
5. S. Mrowec and A. Stoklosa, *Oxidation of. Metals* **3**, 291 (1971).
6. D.T. Hoelzer, B.A. Pint and I.G. Wright, *Journal of Nuclear Materials* 283-287, 1306 (2000).
7. S.N. Busa and G.J. Yurek, *Oxidation of Metals* **36**, 281 (1991).
8. D. Delaunay, A.M. Huntz and P. Lacombe, *Corr. Sci.* **24**(1), 13, (1984).
9. F. Fitzer and J. Schlicting, *International Corrosion Conference* (NACE, Houston, TX, 1981), 604-614.

10. H.E. Evans, D.A. Hilton and R.A. Holm, *Oxidation of Metals* **19**(1), 1, (1983).

11. H.E. Evans, D.A. Hilton, R.A. Holm and S.J. Webster, *Oxidation of Metals* **14**, 235, (1983).

12. A.Kumar and D.L. Douglas, *Oxidation of Metals* **10**(1), 1, (1976).